High-order harmonic generation with controllable temporal coherence generated from a coherently excited medium

Itai Hadas, Liran Hareli, and Alon Bahabad*

Department of Physical Electronics, School of Electrical Engineering, Iby and Aladar Fleischman Faculty of Engineering, Tel-Aviv University, Tel-Aviv 69978, Israel

(Received 7 November 2017; published 16 November 2018)

High harmonic generation has been considered for many years to be a coherent source of upconverted laser radiation. We propose a method for the generation of essentially incoherent high harmonic generation with a controlled degree of temporal coherence, obeying random-walk statistics. This is achieved by a unique combination of single-atom and macroscopic effects involving preparation of the medium in an excited state with coordinate-dependent population inversion and using an intense off-resonant and phase-mismatched pumping.

DOI: 10.1103/PhysRevA.98.053425

I. INTRODUCTION

High harmonic generation (HHG) is an extreme nonlinear process driven with an intense pulsed light source. During HHG, part of the energy of the pump beam is converted to many harmonic orders of the fundamental frequency, emitted in the form of attosecond pulses [1,2]. As HHG is driven with a coherent light source the emitted radiation is also coherent [3,4] which naturally leads to the generation of attosecond pulses and is utilized in attosecond spectroscopy [5] and diffractive coherent imaging [6,7]. However, in some cases there are advantages for using an incoherent light source. For example, to reduce speckle noise in imaging [8,9] or for Fourier-transform spectroscopy [10], which can also suffer from the temporal analog of speckle noise [11]. In 2010 it was suggested that HHG generated in a medium of partially ionized clusters can create incoherent HHG with the degree of coherence depending on the ions density in the clusters [12].

Here we propose a method to generate a unique source of wavelength-scaled HHG (with harmonics in the visible-UV range) with a controlled degree of its temporal coherence, thus alleviating speckle noise. Such a broadband source with a controlled degree of coherence, could be relevant to many applications in imaging and spectroscopy. Additionally such a source can have a bandwidth which is much wider than traditional table-top incoherent sources, and can also be used in pump-probe experiments as it is generated by a pulsed pump laser.

The characteristics of HHG from an excited medium were studied in a series of works, regrading either its spectral properties such as yield [13–17], cut-off energy [18], and double-plateau structure [19,20], its temporal behavior on attosecond time scale [17,21–23], as well as the effect of the orientation of the atomic polarization with respect to the polarization of the pump field [24].

An important concept for analyzing HHG when several bound states are initially populated is the HHG channel, which defines a contribution to the dipole moment of the electron that is associated with ionization and recombination from and to specific bound states [25–27]. We consider a system with only two states—the ground (g) and excited (e) states, for which there are four different channels: gg, eg, ge, and ee (see Fig. 2). We can now use the following form for the dipole moment of a specific qth harmonic, for a specific emitter [26–28]:

$$d(\omega_q) = |a_g|^2 d_{gg}(\omega_q) + a_g^* a_e d_{eg}(\omega_q) + |a_e|^2 d_{ee}(\omega_q) + a_g a_e^* d_{ge}(\omega_q), \quad (1)$$

where $d_{ij}(\omega_q)$ is the Fourier component of the dipole moment matrix element for the ij channel ($i, j \in \{e, g\}$) at frequency $\omega_q = q\omega_0$. Here ω_0 is the HHG pump frequency. a_g and a_e are the probability amplitudes of the bound states. It is obvious that the ge and eg channels are sensitive to the relative phase between the amplitudes of the bound states $\angle(a_e, a_g)$. If we consider now many emitters in the medium, each emitter prepared with a different, random, relative phase then only the radiation emitted by the ge and eg channels would be randomized as well. Thus we term gg and ee as the coherent channels, and eg and ge as the incoherent channels. Strictly speaking the gg and ee channels produce harmonics at frequencies $q\omega_0$ while the ge and eg channels produce harmonics at frequencies $q\omega_0 + \Delta_{eg}$, where Δ_{eg} is the energy difference between the excited and ground state. Under the conditions considered in this work, the coherent and incoherent channels interfere separately, and not with each other. The overall emission thus has a coherent part and an incoherent part, where at the single emitter level the maximal incoherent emission is given when $|a_g| = |a_e| = \sqrt{0.5}$.

II. A SIMPLE MACROSCOPIC MODEL FOR THE GENERATION OF PARTIALLY COHERENT HIGH HARMONICS FROM AN EXCITED MEDIUM

The macroscopic model we consider consists of a medium having a macroscopic phase mismatch Δk [29] (different for each harmonic order) and where the emitters are prepared

*alonb@eng.tau.ac.il

with $\angle(a_e, a_g)$ which is a piecewise constant function along stretches of length Z (we term as coherent grains), assigned with a random value (uniformly distributed between 0 to 2π) at each grain. The overall interaction length is $L = NZ$, where N is a positive integer. Within a grain all radiation channels are coherent, but between grains the eg and ge channels are incoherent. Let us consider the evolution of the field of a given harmonic order along the interaction coordinate. The coherent part of such a field would oscillate periodically due to the phase mismatch as

$$E_c = \mathrm{E}_c \int_0^L e^{i\Delta k z} dz = \mathrm{E}_c e^{-i\Delta k L/2} L \mathrm{sinc}\left(\frac{\Delta k L}{2}\right), \tag{2}$$

where E_c is the amplitude of the coherent emission per emitter, while the incoherent part would grow on average with a random walk statistics, similar to the demonstration of random quasi phase matching (QPM) of second harmonic generation in polycrystalline isotropic materials [30] and to the suggestion for all optical random QPM for HHG [31]. The incoherent part of this field is given by

$$\begin{aligned} E_i &= \mathrm{E}_i \sum_{n=1}^{N} e^{i\phi_n} \int_{(n-1)Z}^{nZ} e^{i\Delta k z} dz \\ &= \mathrm{E}_i e^{-i\Delta k Z/2} Z \mathrm{sinc}\left(\frac{\Delta k Z}{2}\right) \sum_{n=1}^{N} e^{i\tilde{\phi}_n}, \end{aligned} \tag{3}$$

where E_i is the amplitude of the incoherent emission per emitter, ϕ_n is a random phase uniformly distributed between $[0 - 2\pi]$, and $\tilde{\phi}_n = \Delta k Z n + \phi_n$ is still distributed uniformly between $[0 - 2\pi]$. The presence of both coherent and incoherent channels in the field $E = E_c + E_i$ (we remind at a given harmonic order) allows us to continuously tune the temporal coherence level of the emission.

Let us denote

$$E_r = \sum_{n=1}^{N} e^{i\tilde{\phi}_n}. \tag{4}$$

The mean amplitude of this field is given by the well known Rayleigh distribution [32] for which the probability to get the value $|E_r|$ is given by $p(|E_r|) = \frac{2|E_r|}{N} e^{-|E_r|^2/N}$ leading to $\langle |E_r| \rangle = \frac{\sqrt{\pi}}{2}\sqrt{N}$, where the angular brackets stand for the mean value and we assume that $N \gg 1$. Thus the mean amplitude of the incoherent field would be

$$A_i = \langle |E_i| \rangle = |\mathrm{E}_i| Z \mathrm{sinc}\left(\frac{\Delta k Z}{2}\right) \frac{\sqrt{\pi}}{2} \sqrt{N}. \tag{5}$$

Assuming the grains length Z is much smaller than the coherence length $l_c = \pi/\Delta k$ the sinc term above would be approximately 1.

Now, $|E_c|$ evolves periodically with a maximum value of $2|\mathrm{E}_c|/\Delta k$, while A_i monotonously rises and would equal the maximum value of $|E_c|$ at $L = L_{\mathrm{eq}}$ obeying

$$2|\mathrm{E}_c| l_c/\pi = |\mathrm{E}_i| \sqrt{L_{\mathrm{eq}} Z} \sqrt{\pi}/2 \tag{6}$$

giving

$$L_{\mathrm{eq}} = 2\left(\frac{|\mathrm{E}_c|}{|\mathrm{E}_i|}\right)^2 \left(\frac{2}{\pi}\right)^3 \frac{l_c^2}{Z}. \tag{7}$$

If we ignore the ionization dynamics of the upconversion process to approximate the coherent amplitude with $|\mathrm{E}_c| = |a_g|^2 + |a_e|^2 = 1$ and the incoherent amplitude with $|\mathrm{E}_i| = 2|a_g||a_e|$ (with a_g and a_e being the probability amplitudes of the ground and excited states, respectively) we get

$$L_{\mathrm{eq}} = \frac{1}{2|a_g a_e|^2} \left(\frac{2}{\pi}\right)^3 \frac{l_c^2}{Z}. \tag{8}$$

In order to decrease the coherence we thus require a large phase mismatch and long coherent grains Z to set L_{eq} as small as possible. Thus manipulating the macroscopic phase mismatch, the population inversion level, and the grain size, would control the coherence of the total emitted radiation. The last two parameters can be driven all optically as we suggest below. We emphasize that Eq. (8) is valid only for a large number $N \gg 1$ of coherent grains—otherwise increasing Z would actually make the radiation more coherent (which is trivial in the limit where there is just a single coherent grain).

III. A PROPOSED EXPERIMENTAL SETUP

A. The physical system

The actual physical system we suggest is one that we investigated already for the manipulation of coherent HHG [27]. We propose a gas cell containing rubidium (Rb) vapor kept at a pressure of 0.1 Torr and temperature of 220 °C corresponding to atom density of 1.9583×10^{15} atoms/cm^3 with added buffer gas argon at a pressure of 600 Torr to supply the required phase mismatch (e.g., for the 13th harmonic at wavelength of 200 nm, the coherence length is $l_c = 877$ μm). The HHG pump wavelength is 2.6 μm, far off the $D1$ line resonance of rubidium, with pulse duration of 25 fs and intensity of 2×10^{12} W/cm^2 which is too weak for ionizing argon atoms but enough to ionize the ground (and of course excited) state of Rb. This intensity corresponds to HHG cutoff in the 17th harmonic when ionizing from the ground state. The interaction length is taken to be 1 cm.

B. Medium atomic state manipulation

For preparing the required amplitudes and phases of the electronic population of Rb along the interaction direction we can use a coherent control (CC) protocol involving rapid adiabatic passage (RAP) [33,34] to set the required population inversion followed with a nonadiabatic pulse that slightly changes the population while significantly changing the relative phase $\angle(a_e, a_g)$. By illuminating different segments of our medium at slightly different times we can control the relative phase.

In Fig. 1 we present the results of simulations solving the dynamics of a two-level system driven with a light pulse. In each case we applied two pulses in succession. The Rabi frequency Ω (proportional to the amplitude) and detuning $\Delta = \omega_0 - \omega$ (where ω is the time-dependent pulse frequency and ω_0 is the resonance frequency) of the pulses are shown in a continuous and dashed lines, respectively, at the top panel of each case. The first pulse induces RAP. This pulse obeys the adiabatic condition—its amplitude and detuning vary slowly enough to allow adiabatic transfer of the population from

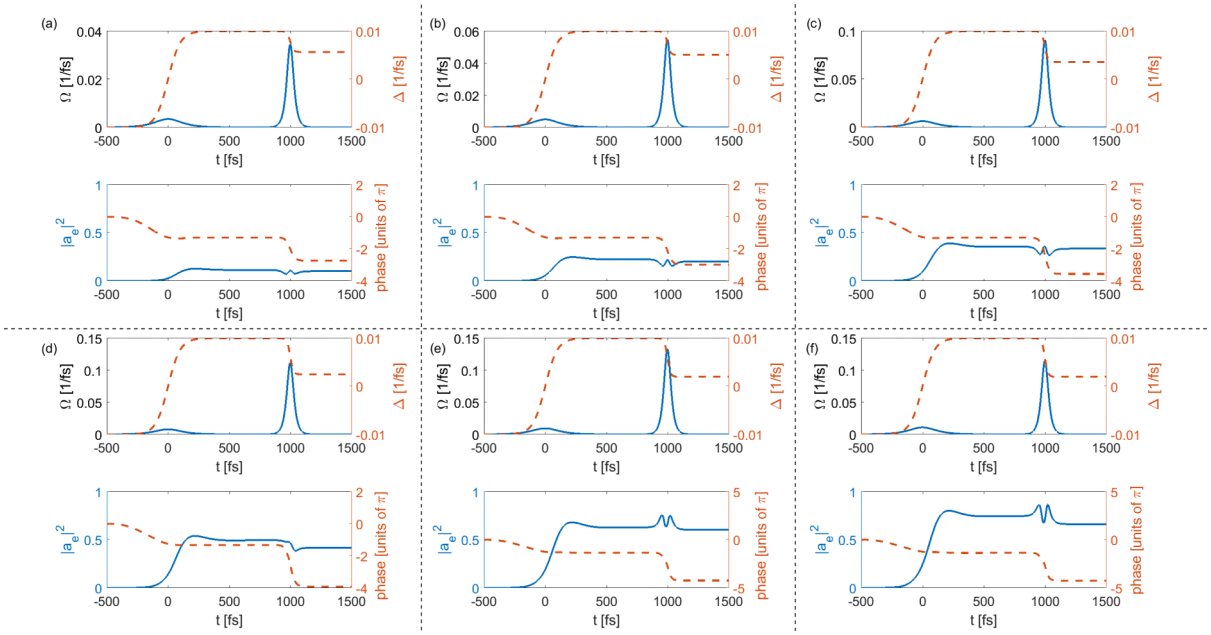

FIG. 1. Coherent control protocol for allowing specific population inversion with fast variation of the relative phase between the levels. In each panel the top figure shows the Rabi frequency Ω (proportional to the amplitude, in a continuous line) and detuning Δ (dashed line) of the coherent control pump. The bottom figure in each panel shows the evolution of the excited state population $|a_e|^2$ (continuous line) and the relative phase between the two levels (dashed line). The different cases are for setting the population of the excited state (within 10%) to values of: 0.1 (a), 0.2 (b), 0.35 (c), 0.45 (d), 0.63 (e), and 0.75 (f).

the ground to the excited state. The spans over which the amplitude and detuning are swept allow us to tune the population inversion at the end of the first pulse. In particular, the RAP pulse is chirped with a slow (adiabatic) frequency sweep around the $D1$ line resonance of the medium. The adiabatic condition [33] is given as $|\dot{\Omega}\Delta - \dot{\Delta}\Omega| \ll 2(\Omega^2 + \Delta^2)^{3/2}$, where the dots stand for time derivatives.

The population of the excited state $|a_e|^2$ and the relative phase $\angle(a_e, a_g)$ between the states are shown in the bottom panel of each case with a continuous and a dashed line, respectively. The second pulse does not obey the adiabatic condition such that although the populations of the levels change only slightly (the excited state population changes by no more than 10% of its value at the end of the adiabatic passage) the relative phase undergoes a fast and relatively large transition at a rate of about $\sim 2\pi/40$ rad/fs. Thus inducing relative random delays between the fields interacting at different locations along the medium where the delays are distributed between 0 and 40 fs would accomplish a smoothed approximation to the desired piecewise constant relative phase function. A 40 fs delay is accomplished with a 12 μm optical delay. Commercial deformable mirrors (DM) with up to about a thousand actuators allow for about 5 μm optical stroke between adjacent actuators and about $\sim$100 μm of total stroke along the whole mirror, which is more than enough for our case, especially if the length along several actuators is imaged to constitute a single coherent grain in the medium. We note that a linear array of deformable actuators (or a DM), programed with the desired $\angle(a_e, a_g)(z)$ pattern and then line focused to the Rb cell, is the best choice for the proposed system. A conceptual configuration is shown in Fig. 2.

C. Geometrical considerations for the CC protocol setup setup

The coherent control (CC) pulse and the HHG pump need to coincide along the pump propagation direction at the time of the rapid strong variation of the relative phase. This means that the surface of the DM cannot be simply imaged with its surface parallel to the propagation line. An arrangement that satisfies this condition is the following: the beam after the DM can be directed at an angle with respect to the interaction line. In this case the HHG pump needs to be set in a spatial mode to match the wave front interaction of the CC beam. The simplest way to accomplish this is to use an HHG pump in the form of a Bessel beam. We note that this can change the particular value of the phase mismatch (for each harmonic order) used in the simulations, but it would have no qualitatively effect—as the phase mismatch can be independently tuned with the pressure of the buffer gas. Furthermore, what is important in this work is the ratio between the square of the coherence length to the coherence grain length [see Eq. (8)] and both can be manipulated. The focusing optics can still be set parallel to the DM surface (all of which are at an angle to the interaction line) as long as the depth of focus of the imaging system is long enough to tolerate the different orientations of the image plane and interaction line. If the depth of focus is too small, we can instead use a nonparallel arrangement of the focusing optics, the DM plane, and the interaction line using the Scheimpflug condition (or principle) [35] allowing us to image the DM surface to the interaction line in focus. Another option to consider is applying a pulse front tilt [36,37] to the CC pulse and stay with the simplest arrangement where all relevant planes are parallel. This option requires further consideration as pulse front tilt is accompanied with spatial dispersion which might affect the coherent control protocol.

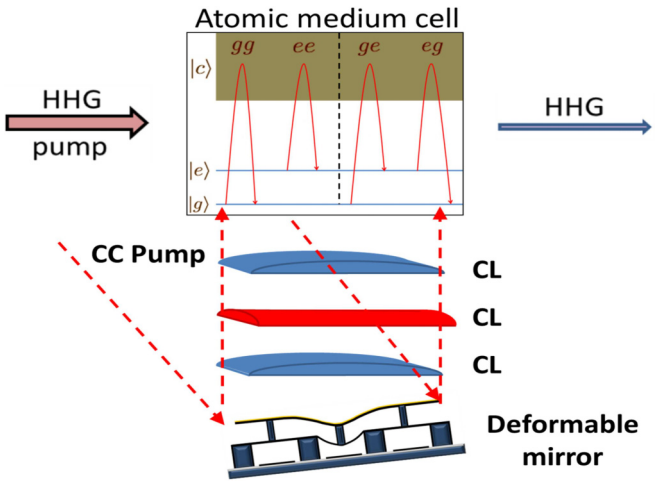

FIG. 2. Proposed system for HHG with controlled temporal coherence. An ionizing HHG pump propagates within an interaction cell containing excited atoms. The atoms are prepared using a coherent control (CC) pump reflected of a deformable mirror (DM) whose surface is imaged and line focused using cylindrical lenses (CL) to the interaction cell. $|g\rangle$ ($|e\rangle$) is the ground (first excited) state of the atom, $|c\rangle$ represents continuum states. HHG is generated in channels, each includes ionization of an electron from a bound state to the continuum and its recombination into the same or another bound state, e.g., the ge channel involves ionization from the ground state and recombination into the excited state. The dashed line separates the coherent channels gg and ee from the possibly incoherent channels ge and eg.

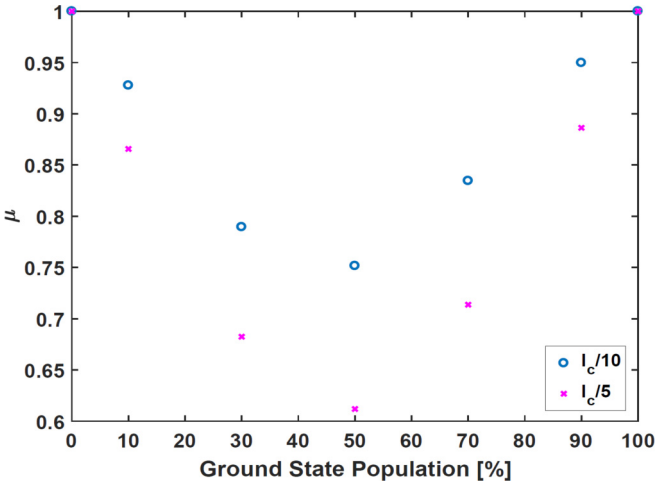

FIG. 3. Integral degree of coherence μ as a function of the ground state population calculated for the total field of HHG emission. The blue circles are the results for coherent grains of length $Z = l_c/10$ and the magenta x's are the results for coherent grains of length $Z = l_c/5$, where l_c is the coherence length of the 13th harmonic.

IV. SIMULATION RESULTS

The evolution of the ionizing HHG pump through the medium has been simulated using the propagation equation of Geissler *et al.* [38] with an additional dispersion term for the buffer gas. HHG has been simulated by solving the one-dimensional Schrödinger equation using the split step method. The initial state for the solution of the Schrödinger equation at every calculated propagation coordinate is set through the desired electronic population distribution and desired relative phase function $\angle(a_e, a_g)(z)$.

We investigated different initial population configurations in which the ground state population is $|a_g|^2 = 0.1,\ 0.3,\ 0.5,\ 0.7,\ 0.9$. For each population configuration we used two coherent grain lengths $Z = l_c/5,\ l_c/10$. Since the relative electronic phases are random we investigated the stochastic properties of the propagation by using an ensemble of 100 relative phases for each case of specific initial population and grain length.

For each such case a measure of the temporal coherence was calculated in the form of an integral effective degree of coherence [39,40], defined as

$$\mu^2 = \frac{1}{2\pi E_0^2}\int\int_{-\infty}^{\infty} |\Gamma(t_1, t_2)|^2 dt_1 dt_2, \tag{9}$$

where $\Gamma(t_1, t_2) = \langle E^*(t_1)E(t_2)\rangle$ is the covariance matrix of the ensemble of generated pulses (the angular brackets denote an ensemble average and $E(t)$ is the total field of the HHG emission containing all harmonic orders), $E_0 = \int_{-\infty}^{\infty} I(t)dt$, and $I(t) = \Gamma(t, t)$. μ values can vary between 0 and 1, when 1 means total coherence and 0 means total incoherence of the interaction. The results of this calculation, for all cases of ground state population and two cases for the length of the coherent grains, are shown in Fig. 3, which constitutes the major result of this work. The length of the coherent grain is given in units of the coherence length of the 13th harmonic order which is equal to 877 μm in our model. The range of coherence lengths for the different harmonics in the field starting from the 5th is 2115 to 602 μm for the cutoff 17th harmonic. First we notice that having a longer grain length reduces the coherence. This is the result of having the incoherent part of the emission following a random walk with a longer step size. Additionally, it is clear that the coherence is minimal when the electron population is equally shared between the ground and excited states, supplying the largest incoherent emission as is clear from Eq. (1). Both these observations agree well with Eq. (8). It is interesting to note that the degree of coherence is slightly asymmetric as a function of the ground state population. For example the coherence is larger for $|a_g|^2 = 0.9$ compared with the complementary case of $|a_g|^2 = 0.1$. This is due to the ionization dynamics that take place when the HHG pump interacts with the emitters. The excited state depletes faster than ground state and so the contribution of the coherent ee channel is slightly less significant than that of the coherent gg channel, leading to the observed asymmetry.

In Fig. 4 we show a comparison of the HHG field for the coherent case ($\mu = 1$) against a member of the ensemble of incoherent pulses (for initial ground state population of 50% and $\mu \approx 0.6$). The phase jumps of the incoherent pulse attest to the reduced temporal coherence compared with the coherent emission. Also notice that any single pulse of the ensemble of incoherent pulses might be of lower or higher energy compared to the coherent case, while the behavior of the ensemble average field is discussed below.

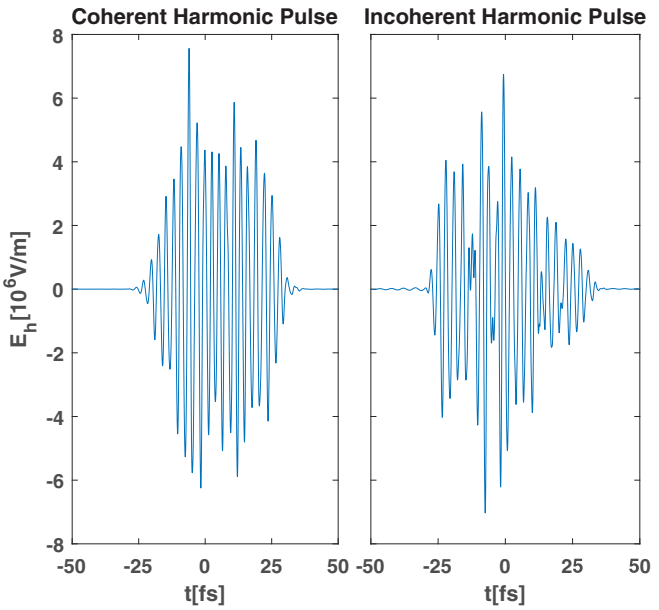

FIG. 4. A comparison between the high harmonic fields of a coherent pulse ($\mu = 1$) and a member of the ensemble of incoherent pulses ($\mu \approx 0.6$).

Next we examine the overall high-harmonic spectrum at the end of the interaction length for the different cases considered here. The results are shown in Fig. 5(a). The most obvious observation as the radiation loses coherence (as the population distribution becomes more balanced) is the disappearance of ordered structure in the spectrum, that is the ability to define specific harmonic orders, as the whole spectrum becomes flatter. This is a signature of the increasing variance for the spectrum of each member of the ensemble. Additionally, most of the spectrum increases in intensity, owing to the fact that less radiation destruct coherently due to phase mismatch. This is seen more clearly in Fig. 5(b) showing the evolution of the 13th harmonic along the Rb cell. For high coherence configurations the oscillations associated with phase mismatch precludes buildup of the emitted radiation, a condition which is alleviated as the radiation becomes incoherent and contains an approximately linear buildup of the emission as a function of the coordinate. The buildup is higher when Z is longer as anticipated. This type of evolution should be wide band in nature, and not restricted to a single harmonic. This fact is clearly seen in Fig. 5(c) showing the evolution of all harmonic orders (until the cutoff) for the case of lowest coherence. As in our proposed system both the initial population and relative phase can be determined all

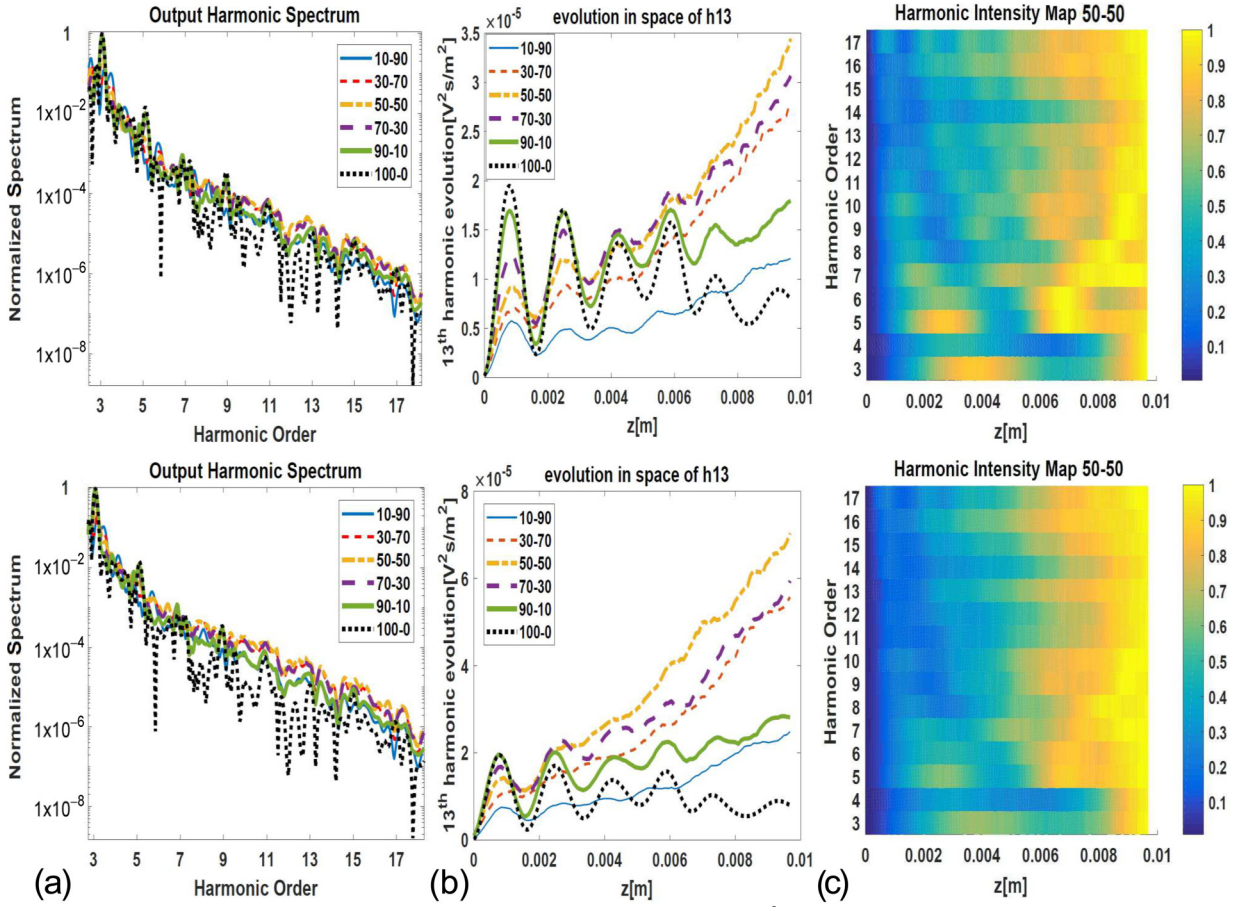

FIG. 5. Simulation results of HHG propagation in the proposed system. (a) Harmonic spectrum for different initial electron population distributions between the ground and excited states, e.g., 100−0 stands for totally populated ground state. (b) Evolution of the intensity of the 13th harmonic order along the interaction length for different population distributions. (c) Evolution of all harmonic orders for 50–50 population distribution. The length of the coherent grains is (top) $Z = l_c/10$, (bottom) $Z = l_c/5$.

optically, the coherence and enhancement of the radiation can be controlled precisely and easily. We note that the existence of commercial deformable mirrors with 1 kHz refresh rates allows us to pump the system with up to 1 kHz repetition rate laser such that each pulse experience a unique random relative phase function. In this case 0.1 s integration time of any measurement (setting the ensemble size to 100) would correspond to the ensemble average presented here. We would like to add that the broadband incoherent buildup of the radiation in our case serves as an alternative to the much more complicated suggestion using accelerating light [41].

V. CONCLUSIONS

To conclude, despite the prevalent understanding that HHG is a coherent process leading to the emission of highly coherent radiation, we have suggested to apply coordinate-dependent rapid adiabatic passage protocol to coherently control and prepare an excited medium to be subsequently pumped with an ionizing off-resonant pulse for the generation of HHG with a controlled level of temporal coherence. The proposed system is pumped with a relatively long wavelength HHG pump pulse, leading to broadband emission spanning the UV-visible range. We note that here we suggested to realize the incoherent radiation with simple constant-step random walk statistics, however the same system can easily be used to apply other forms of random walks such as Levy flight [42].

ACKNOWLEDGMENTS

This work was supported by the Israeli Science Foundation, Grant No. 1233/13 and by the Wolfson foundation's High Field Physics and Attosecond Science Grant.

[1] H. Kapteyn, O. Cohen, I. Christov, and M. Murnane, Harnessing attosecond science in the quest for coherent x-rays, Science **317**, 775 (2007).

[2] P. B. Corkum and F. Krausz, Attosecond science, Nat. Phys. **3**, 381 (2007).

[3] M. Bellini, C. Lyngå, A. Tozzi, M. B. Gaarde, T. W. Hänsch, A. L'Huillier, and C.-G. Wahlström, Temporal Coherence of Ultrashort High-Order Harmonic Pulses, Phys. Rev. Lett. **81**, 297 (1998).

[4] P. M. Paul, E. S. Toma, P. Breger, G. Mullot, F. Augé, Ph. Balcou, H. G. Muller, and P. Agostini, Observation of a train of attosecond pulses from high harmonic generation, Science **292**, 1689 (2001).

[5] F. Krausz and M. Ivanov, Attosecond physics, Rev. Mod. Phys. **81**, 163 (2009).

[6] R. L. Sandberg, A. Paul, D. A. Raymondson, S. Hädrich, D. M. Gaudiosi, J. Holtsnider, I. Tobey Ra'anan, O. Cohen, M. M. Murnane, H. C. Kapteyn *et al.*, Lensless Diffractive Imaging Using Tabletop Coherent High-Harmonic Soft-X-Ray Beams, Phys. Rev. Lett. **99**, 098103 (2007).

[7] H. N. Chapman and K. A. Nugent, Coherent lensless x-ray imaging, Nat. Photon. **4**, 833 (2010).

[8] B. Redding, M. A. Choma, and H. Cao, Speckle-free laser imaging using random laser illumination, Nat. Photon. **6**, 355 (2012).

[9] J. W. Goodman, *Speckle Phenomena in Optics: Theory and Applications* (Roberts and Company Publishers, 2007).

[10] S. P. Davis, M. C. Abrams, and J. W. Brault, *Fourier Transform Spectrometry* (Academic, New York, 2001).

[11] T. Steinle, F. Neubrech, A. Steinmann, X. Yin, and H. Giessen, Mid-infrared Fourier-transform spectroscopy with a high-brilliance tunable laser source: Investigating sample areas down to 5 μm diameter, Opt. Express **23**, 11105 (2015).

[12] D. F. Zaretsky, Ph. Korneev, and W. Becker, High-order harmonic generation in clusters irradiated by an infrared laser field of moderate intensity, J. Phys. B: At. Mol. Opt. Phys. **43**, 105402 (2010).

[13] A. K. Gupta and D. Neuhauser, Control of harmonic generation by initial-state preparation, Chem. Phys. Lett. **290**, 543 (1998).

[14] B. Wang, T. Cheng, X. Li, P. Fu, S. Chen, and J. Liu, Pulse-duration dependence of high-order harmonic generation with coherent superposition state, Phys. Rev. A **72**, 063412 (2005).

[15] P. M. Paul, T. O. Clatterbuck, C. Lyngå, P. Colosimo, L. F. DiMauro, P. Agostini, and K. C. Kulander, Enhanced High Harmonic Generation from an Optically Prepared Excited Medium, Phys. Rev. Lett. **94**, 113906 (2005).

[16] I. A. Ivanov and A. S. Kheifets, High harmonics generation from excited states of atomic lithium, J. Phys. B: At. Mol. Opt. Phys. **41**, 115603 (2008).

[17] J.-G. Chen, Y.-J. Yang, S.-L. Zeng, and H.-Q. Liang, Generation of intense isolated sub-40-as pulses from a coherent superposition state by quantum path control in the multicycle regime, Phys. Rev. A **83**, 023401 (2011).

[18] Y.-J. Yang, J.-G. Chen, F.-P. Chi, Q.-R. Zhu, H.-X. Zhang, and J.-Z. Sun, Ultrahigh harmonic generation from an atom with superposition of ground state and highly excited states, Chin. Phys. Lett. **24**, 1537 (2007).

[19] A. Sanpera, J. B. Watson, M. Lewenstein, and K. Burnett, Harmonic-generation control, Phys. Rev. A **54**, 4320 (1996).

[20] J. B. Watson, A. Sanpera, X. Chen, and K. Burnett, Harmonic generation from a coherent superposition of states, Phys. Rev. A **53**, R1962 (1996).

[21] V. A. Antonov, Y. V. Radeonychev, and O. Kocharovskaya, Formation of a Single Attosecond Pulse Via Interaction of Resonant Radiation with a Strongly Perturbed Atomic Transition, Phys. Rev. Lett. **110**, 213903 (2013).

[22] S. Chelkowski, T. Bredtmann, and A. D. Bandrauk, High-order-harmonic generation from coherent electron wave packets in atoms and molecules as a tool for monitoring attosecond electrons, Phys. Rev. A **85**, 033404 (2012).

[23] S. Chelkowski, T. Bredtmann, and A. D. Bandrauk, High-harmonic generation from a coherent superposition of electronic states: Controlling interference patterns via short and long quantum orbits, Phys. Rev. A **88**, 033423 (2013).

[24] V. Averbukh, High-order harmonic generation by excited helium: The atomic polarization effect, Phys. Rev. A **69**, 043406 (2004).

[25] C. Figueira de Morisson Faria, M. Dörr, and W. Sandner, Importance of excited bound states in harmonic generation, Phys. Rev. A **58**, 2990 (1998).

[26] J. Bao, W. Chen, Z. Zhao, and J. Yuan, High-order harmonic generation from coherently excited molecules, J. Phys. B: At. Mol. Opt. Phys. **44**, 195601 (2011).

[27] I. Hadas and A. Bahabad, Macroscopic Manipulation of High-Order-Harmonic Generation Through Bound-State Coherent Control, Phys. Rev. Lett. **113**, 253902 (2014).

[28] P. M. Kraus, S. Bin Zhang, A. Gijsbertsen, R. R. Lucchese, N. Rohringer, and H. J. Wörner, High-Harmonic Probing of Electronic Coherence in Dynamically Aligned Molecules, Phys. Rev. Lett. **111**, 243005 (2013).

[29] A. Bahabad, M. M. Murnane, and H. C. Kapteyn, Quasi-phase-matching of momentum and energy in nonlinear optical processes, Nat. Photon. **4**, 570 (2010).

[30] M. Baudrier-Raybaut, R. Haidar, Ph. Kupecek, Ph. Lemasson, and E. Rosencher, Random quasi-phase-matching in bulk polycrystalline isotropic nonlinear materials, Nature (London) **432**, 374 (2004).

[31] A. Bahabad, O. Cohen, M. M. Murnane, and H. C. Kapteyn, Quasi-periodic and random quasi-phase matching of high harmonic generation, Opt. Lett. **33**, 1936 (2008).

[32] P. Beckmann, Rayleigh distribution and its generalizations, Radio Sci. J. Res. NBS/USNC-URSI, 68D, **9**, 927 (1962).

[33] N. V. Vitanov, Th. Halfmann, B. W. Shore, and K. Bergmann, Laser-induced population transfer by adiabatic passage techniques, Annu. Rev. Phys. Chem. **52**, 763 (2001).

[34] B. W. Shore, Coherent manipulations of atoms using laser light, Acta Phys. Slovaca: Rev. Tutorials **58**, 243 (2008).

[35] W. Smith, *Modern Optical Engineering, 4th Ed.*, McGraw-Hill series on optical and electro-optical engineering (McGraw-Hill, New York, 2007).

[36] S. Akturk, X. Gu, E. Zeek, and R. Trebino, Pulse-front tilt caused by spatial and temporal chirp, Opt. Express **12**, 4399 (2004).

[37] P. Bowlan and R. Trebino, Extreme pulse-front tilt from an etalon, J. Opt. Soc. Am. B **27**, 2322 (2010).

[38] M. Geissler, G. Tempea, A. Scrinzi, M. Schnürer, F. Krausz, and T. Brabec, Light Propagation in Field-Ionizing Media: Extreme Nonlinear Optics, Phys. Rev. Lett. **83**, 2930 (1999).

[39] G. Genty, A. T. Friberg, and J. Turunen, Chapter two-coherence of supercontinuum light, Prog. Opt. **61**, 71 (2016).

[40] C. Iaconis, V. Wong, and I. A. Walmsley, Direct interferometric techniques for characterizing ultrashort optical pulses, IEEE J. Sel. Top. Quantum Electron. **4**, 285 (1998).

[41] A. Bahabad, M. M. Murnane, and H. C. Kapteyn, Manipulating nonlinear optical processes with accelerating light beams, Phys. Rev. A **84**, 033819 (2011).

[42] P. Barthelemy, J. Bertolotti, and D. S. Wiersma, A Lévy flight for light, Nature (London) **453**, 495 (2008).